GEODYNAMICS & TECTONOPHYSICS
Published by the Institute of the Earth's Crust, Siberian Branch, Russian Academy of Sciences

PALEOGEODYNAMICS

2023 VOLUME 14 ISSUE 5 ARTICLE 0718

ISSN 2078-502X

DOI: 10.5800/GT-2023-14-5-0718

PROVENANCE OF THE PERMIAN-TRIASSIC RED BEDS FROM THE EASTERN PART OF THE MOSCOW BASIN, EAST EUROPEAN PLATFORM: U-Pb LA-ICP-MS AND RAMAN SPECTROSCOPY DETRITAL ZIRCON DATA

A.V. Chistyakova [1,2]✉, **R.V. Veselovskiy** [1,2], **V.B. Khubanov** [3], **A.V. Ivanov** [4], **A.E. Marfin** [4], **N.V. Bryanskiy** [4,5], **V.K. Golubev** [6,7]

[1] Lomonosov Moscow State University, 1 Leninskie Gory, Moscow 119991, Russia
[2] Schmidt Institute of Physics of the Earth, Russian Academy of Sciences, 10-1 Bolshaya Gruzinskaya St, Moscow 123242, Russia
[3] Dobretsov Geological Institute, Siberian Branch of the Russian Academy of Sciences, 6a Sakhyanova St, Ulan-Ude 670047, Republic of Buryatia, Russia
[4] Institute of the Earth's Crust, Siberian Branch of the Russian Academy of Sciences, 128 Lermontov St, Irkutsk 664033, Russia
[5] Vinogradov Institute of Geochemistry, Siberian Branch of the Russian Academy of Sciences, 1a Favorsky St, Irkutsk 664033, Russia
[6] Borissiak Paleontological Institute, Russian Academy of Sciences, 123 Profsoyuznaya St, Moscow 117647, Russia
[7] Kazan Federal University, 18 Kremlyovskaya St, Kazan 420008, Russia

ABSTRACT. We present the first systematic results of U-Pb LA-ICP-MS dating of detrital zircons from 12 samples representing different stratigraphic levels of 5 sections of the Permian-Triassic rocks, located within the eastern part of the Moscow basin (syneclise) – Zhukov ravine, Astashikha, Nedubrovo, Balebikha and Klykovo. It is shown that the accumulation of the Upper Permian and Lower Triassic terrigenous complexes occurred under the influence of competing sources with two contrasting provenance signals with Neoproterozoic (Vendian)-Paleozoic and Paleo-Mesoproterozoic ages. The identified provenance signal patterns were used to detail the correlation and stratigraphic subdivision of the Permian-Triassic terrigenous complex of the Moscow basin. Raman spectroscopy of detrital zircon, first applied to the Permian-Triassic rocks of the East European Platform, made it possible to identify sedimentary complexes of a relatively older terrigenous basin as a separate source of zircons, which experienced superimposed thermal impact in the Vendian-Cambrian time (~500–600 Ma).

KEYWORDS: detrital zircon; U-Pb LA-ICP-MS dating; Raman spectroscopy; Permian; Triassic; East European Platform

FUNDING: The study was supported by the RSF, grant 22-27-00597. The studies were carried out using the "Analytical Study of the Early History of the Earth" Shared Research Facilities (SRF) of the IPGG RAS (Saint Petersburg), "GeoSpectrum" SRF of the GIN SB RAS (Ulan-Ude), "Geodynamics and Geochronology" SRF of the IEC SB RAS (Irkutsk), "Petrophysics, Geomechanics and Paleomagnetism" SRF of the IEPh RAS (Moscow), and "IGEM-Analytics" SRF of the IGEM RAS (Moscow).

RESEARCH ARTICLE

Correspondence: Alvina V. Chistyakova, alvina.tch@gmail.com

Received: February 14, 2023
Revised: May 10, 2023
Accepted: May 12, 2023

FOR CITATION: Chistyakova A.V., Veselovskiy R.V., Khubanov V.B., Ivanov A.V., Marfin A.E., Bryanskiy N.V., Golubev V.K., 2023. Provenance of the Permian-Triassic Red Beds from the Eastern Part of the Moscow Basin, East European Platform: U-Pb LA-ICP-MS and Raman Spectroscopy Detrital Zircon Data. Geodynamics & Tectonophysics 14 (5), 0718. doi:10.5800/GT-2023-14-5-0718

Supplementary files: Chistyakova_et_al_2023_Suppl_1.pdf, Chistyakova_et_al_ 2023_Suppl_2.xlsx, Chistyakova_et_al_ 2023_Suppl_3.pdf, Chistyakova_et_al_ 2023_Suppl_4.pdf

1. INTRODUCTION

At the Paleozoic-Mesozoic boundary, there occurred a planetary-scale geosystem reworking that affected also the East European Platform [Lozovsky et al., 2016; Kuleshov et al., 2019]. Its paleogeographic conditions in the period considered are closely related to both climate fluctuations and paleotectonic aspects. The evolution of the Paleo-Urals, marked by intensive reactivation at the Permian-Triassic boundary [Puchkov, 2010; Arefiev, 2016b], is considered to be one of the key factors determining the sediment removal into the basin of the Russian Platform (Russian Basin) at that time.

The Upper Permian – Lower Triassic complex of the East European Platform is accessible for study in numerous outcrops along the eastern and northeastern parts of the Moscow syneclise (Fig. 1). The Paleozoic-Mesozoic central and eastern parts of the East European Platform were extensive lowland, characterized by poorly dissected relief and unstable hydrogeological regime, wherein were formed laterally discontinuous red-colored and variegated sandstone, siltstone and clay beds with paleosoil horizons and thin interlayers of gray-colored marls and limestones. Thin horizontal bedding and a high share of pelitic fraction in the described rocks indicate that sediment deposition occurred under quiet hydrodynamical conditions, though the plain covered by soft sludge-like sediment was easily cut by both permanent and temporary stream channels. Thus, ether increase or decrease in runoff from remote upland catchments, for example, from the western slopes of the Paleo-Urals orogen, had a direct impact on sedimentation character [Ivakhnenko, 2001; Kiselev et al., 2012].

The Upper Permian and Lower Triassic continental complexes of the Russian Platform are characterized by cyclicity [Arefiev, 2016a], which in the first approximation is typical of the lithologic composition of formation members. A frequent alternation of rocks with iron oxide content (red-colored) and without it (bluish-gray color) indicates a rapid change in sedimentary environment conditions, most clearly represented by the oxygen saturation degree. Such sedimentation character is in conformity with a model of vast alluvial lowland, submerged almost entirely during the flood seasons and fallen dry during low-water periods. Oscillation of heavy mineral compositions was reported in [Strok, Trofimova, 1976], but the first detailed studies based on the modern stratigraphic scheme were only made for single cross-sections [Arefiev et al., 2016b]. The revealed regularities reflect the competition between two distributive provinces for the discharge area. However, the analysis of heavy minerals allows a fairly wide variability in the interpretation of direct source areas, especially in case of a prevalence of garnet-zircon association [Lozovsky, Esaulova, 1998], and their relative contribution to a total debris volume.

Of further relevance is the problem of stratification and correlation of the Permian-Triassic continental sediments of the East European Platform which has arisen since the very beginning of their systematic studies in the early 20th century. Due to the known features of the formation of continental sedimentary units, such as intraformational hiatuses, lateral facies variation, lack of the regional lithological markers and many others, both global and intrabasin correlation of the Permian-Triassic cross-sections of the Russian Platform were and are the subject of lively discussions because of which the stratigraphic scheme of the Permian to Triassic sedimentary complex was repeatedly updated over the last decades [Golubev, 2016; Lozovsky, Novikov, 2016]. A globally used method to reconstruct the distributive provinces (debris flow source areas) in the sedimentary basins with U-Pb detrital zircon dating is a relatively new and effective tool of intrabasin stratigraphic correlation and paleogeographic reconstruction, but until recently, such studies were not performed for the Permian-Triassic complex of the central Russian Platform. The reconnaissance we made in 2019 for two cross-sections of the eastern part of the Moscow syneclise – Zhukov ravine and Nedubrovo – showed a principally new possibility of using this method to specify the stratigraphic position of the cross-sections of controversial age [Chistyakova et al., 2020]. Therefore, the systematic studies, aimed at identifying the source areas and estimating their share in the total volume of debris removal into the Moscow sedimentary basin in the Late Permian and Early Triassic, are relevant not only for paleogeographic reconstructions of the East European Platform and its borders in the time interval considered but also for solving tasks of stratigraphic correlation and stratification of sediments.

The authors [Resentini et al., 2020] were able to obtain additional characteristics for the Lower Cretaceous debris flow source areas near the Zambezi River delta (South Africa) using Raman spectroscopy of zircon grains. This technique is based on the relationship between the degree of metamictization in zircon and accumulated α-radiation dose which, in turn, depends upon zircon age and its U and Th concentrations. The degree of metamictization in zircon is reflected in the number of Raman spectra characteristics, particularly in position of the $\nu_3(SiO_4)$ peak, occurring for the grains with a high degree of crystallinity at a level of 1008 cm^{-1}. However, the crystalline structure of zircon can be fully or partially restored during thermal annealing without participation of fluids [Nasdala et al., 2001]. In this case, there can be no loss of radiogenic lead, and the degree of metamictization in zircon may differ significantly from that expected for corresponding age, thus making it possible to trace the imposed low-temperature events which affected zircon after crystallization [Resentini et al., 2020]. According to the experimental data [Härtel et al., 2021], the $\nu_3(SiO_4)$ Raman peak shift occurs at temperatures ranging from 330 to 370 °C, though [Pidgeon, 2014] suggests that partial restoration of zircon crystallinity without disturbance of the U-Pb isotopic system can take place even at lower temperatures ~130–320 °C.

The present study is mainly aimed at actualizing and detailing the existing ideas about debris flow source areas in the Moscow sedimentary basin in the Late Paleozoic – Early Mesozoic and revealing dynamics of alternation of distributive provinces within the eastern part of the Moscow

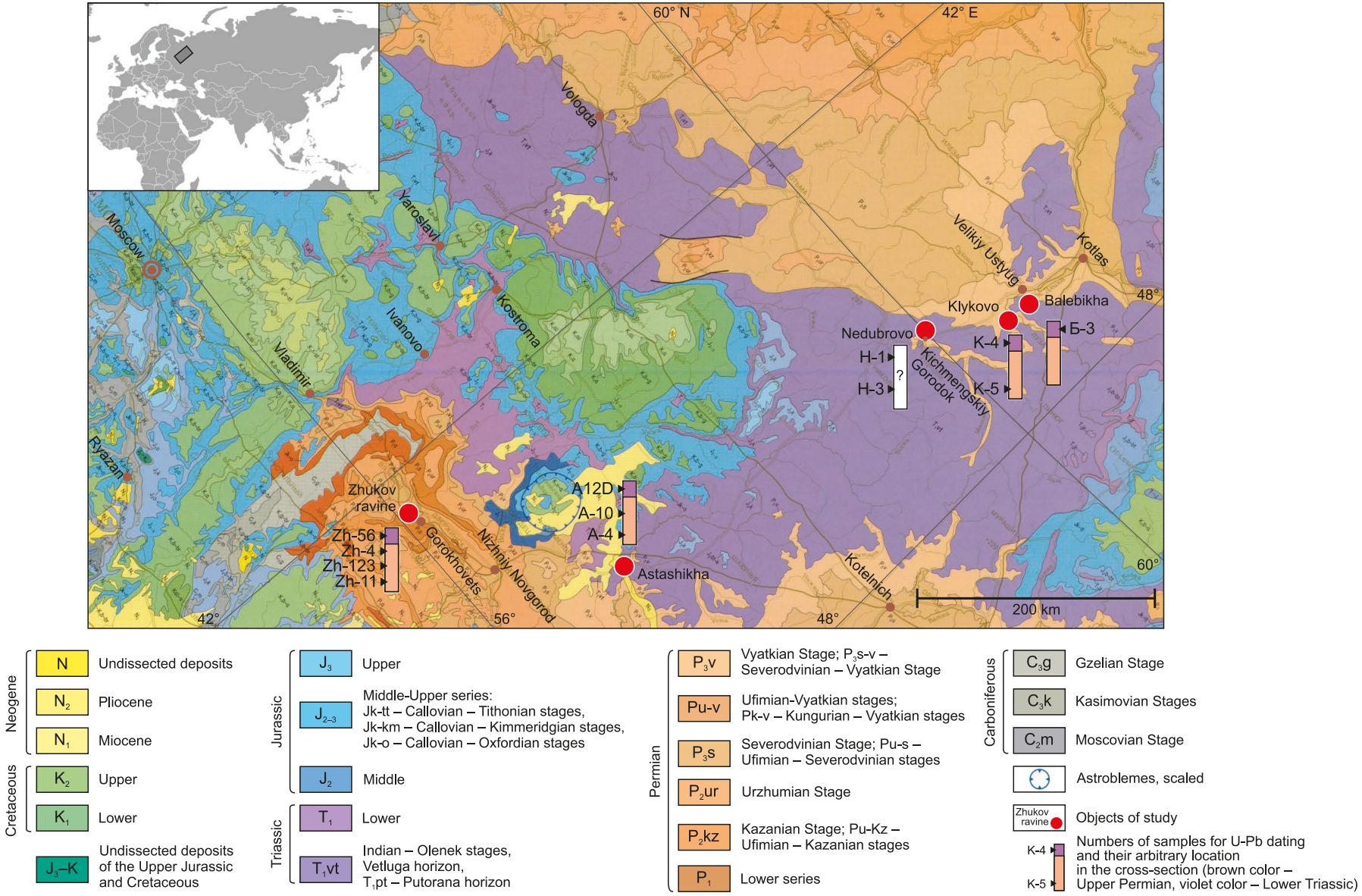

Fig. 1. A fragment of the 1:2500000-scale geological map of Russia and adjacent water areas [Petrov, 2012] for the Moscow basin with the studied sections. Black rectangle in the inset shows the study area. See [Chistyakova et al., 2020] for a sketch tectonic map of the East European Platform.

syneclise from the results of U-Pb dating and Raman spectroscopy of detrital zircon grains in the context of obtaining additional constraints for regional stratigraphic correlation.

2. OBJECTS OF STUDY

The Permian to Triassic cross-sections of the Russian Platform contain many obvious and hidden local breaks, which implies that stratigraphic cross-sectional correlation remains controversial. However, for the Zhukov ravine section (Vladimir Region), the stratigraphic continuity of the Upper Permian to Triassic deposits is sufficiently substantiated and reliable due to high paleontological data informativity [Golubev, 2019], so that it is considered to be a reference section for the Permian to Triassic rocks not only of the Moscow syneclise but also of the East European Platform as a whole [Golubev et al., 2012]. This section plays a key role in ongoing research. We also studied four representative Permian to Triassic section of the Russian Platform (Fig. 1): Astashikha (Nizhny Novgorod Region), and Nedubrovo, Klykovo and Balebikha (Vologda Region). The cross-sections mentioned are comprehensively characterized by the modern lithological-paleontological, paleomagnetic and isotopic-geochemical data [Lozovsky, Esaulova, 1998; Golubev et al., 2012; Arefiev et al., 2015, 2016a, 2016b, 2017; Lozovsky et al., 2016; Kuleshov et al., 2019; Fetisova et al., 2018, 2022].

The Zhukov ravine is located near Gorokhovets (Fig. 1) and dissects the steep right slope of the Klyazma River valley. A series of outcrops on the ravine slopes forms the composite Zhukov ravine section of more than 45 m in thickness. The Permian-Triassic boundary is traditionally identified therein with the base of the Vokhmian horizon. Four samples for U-Pb zircon dating were taken from the sandstone layers in the Nefedovian (sample Zh-11), Zhukovian (samples Zh-123 and Zh-4) and Vokhmian (sample Zh-56) horizons (Table 1).

The section of the Astashikha locality is situated on the right bank of the Vetluga River (Fig. 1). The samples for detrital zircon dating were taken at three different levels (Table 1): upper Zhukovian (sample A-4) and Vokhmian (samples A-10 and A12D) horizons. The Permian-Triassic boundary section between the A-10 and A12D sampling levels is derived from the isotopic-geochemical data [Arefiev et al., 2017].

The natural outcrop of the Nedubrovo locality lies within the village of the same name on the left bank of the Kichmenga River. The rocks of this section became of particular importance with the advent of reliable age estimation based on a discovered interval of anomalous paleomagnetic directions [Fetisova et al., 2018]. Unfortunately, the results of paleontological and isotopic-geochemical [Arefiev et al., 2015, 2017; Lozovsky et al., 2016; Kuleshov et al., 2019] and magnetostratigraphic [Fetisova et al., 2018] studies do not clarify the stratigraphic position of the Nedubrovo sediments in the regional cross-section: according to the biostratigraphic and isotopic-geochemical data, the Nedubrovo section is situated in the lower part of the Lower Vokhmian Subhorizon, and the magnetostratigraphic data imply that it is located in the lower part of the Zhukovian horizon (Table 1). The samples for detrital zircon dating were taken from the lower (sample H-3) and upper (sample H-1) parts of the section.

The sections of the Klykovo and Balebikha localities are usually considered as composite sections of the Permian to Triassic sediments in the lower reaches of the Yug River

Table 1. A brief description of the selected samples

Section	Coordinates (N, E)	Sample	Layer No.	Description
Zhukov ravine (reference)	56.179337° 42.641613°	Zh-56	7 (outcrop 1029) [Golubev et al., 2012]	Brown-gray fine-to-middle-grained inhomogeneously consolidated polymictic sandstones. Sandstones, cross-bedded in the lower part and horizontally bedded in the upper; there are thin interlayers of brown clays and immature paleosoils
		Zh-4	A9 (outcrop 1029) [Golubev et al., 2012]	The sample is a gray gravelite infill: gray fine-to-middle-grained massive sandstones. Gravel in the sampled layer is composed of subisometric, often flat, angular marl fragments
	56.179339° 42.641035°	Zh-123	6 (outcrop 1151) [Golubev et al., 2012]	Gray fine-grained massive polymictic sandstones with rare inclusions of gray marl gravel
	56.179759° 42.636625°	Zh-11	27 (outcrop 1023) [Golubev et al., 2012]	Gray-yellow middle-grained poorly cemented oligomictic sandstones interlayered with mottled clays. The lower boundary of the layer is sharp and erosional
Astashikha	56.920614° 45.335863°	A12D A-10 A-4		Reddish-brown middle-to-fine-grained polymictic sandstones
Nedubrovo	60.04521° 45.74047°	H-1	11 [Arefiev et al., 2015]	Gray siltstone lenses in the upper part of the layer
		H-3	4 [Arefiev et al., 2015]	Gray-brown thin-slabby aleurosandstones
Klykovo	60.573175° 46.414272°	K-4	6 (Klykovo-III lens) [Arefiev et al., 2016a]	Grayish-brown fine-to-middle-grained polymictic sandstones with gravel admixture
	60.573117° 46.416853°	K-5	1 (Klykovo-I lensI) [Arefiev et al., 2016a]	Greenish-gray fine-to-middle-grained poorly cemented polymictic sandstones
Balebikha	60.726090° 46.388317°	Б-3	9 [Arefiev et al., 2016b]	Greenish-reddish middle-grained polymictic sands with bluish-gray gravelite lenses of the lower part of the layer

and in Malaya Severnaya Dvina River basin, respectively [Arefiev et al., 2016a, 2016b]. However, the Lower Triassic Vokhmian horizon, composed of coarse-grained alluvial channel deposits, occurs only near Klykovo and Balebikha localities. It is worthy of note that these two composite sections, comparable to each other, were earlier involved in the detailed heavy mineral analysis [Arefiev et al., 2016b]. The samples for detrital zircon dating were taken in the Balebikha section from the Vokhmian horizon (sample Б-3) and in the Klykovo section from the Vokhmian horizon (sample К-4) and from the lower part of the Nefedovian horizon (sample К-5) (Table 1).

Coordinates of the sampling sites and a brief lithological characteristic of the corresponding rocks are shown in Table 1.

3. RESEARCH METHODS

3.1. U-Pb LA-ICP-MS zircon dating

A representative number of zircon grains (70–150) was obtained for each of 12 sandstone and aleurosandstone samples characterizing different stratigraphic levels of five representative Permian-Triassic sections of the Russian Platform (Fig. 1; Table 1). The grains belong to a 50–200 μm fraction. Zircon was extracted using standard heavy liquid and electrical separation techniques in mineralogical laboratories of the IPGG RAS and IGEM RAS. Cathodoluminescent (CL) images were obtained for each sample (Suppl. 1 on article page online). CL color images were obtained for two samples (Zh-123, A12D) using Cameca MS-46 electron microprobe (IGEM RAS). TESCAN VEGA 3 (IPGG RAS) and TESCAN MIRA IV (IPhE RAS) scanning electron microscopes equipped with panchromatic detectors were used to obtain CL images for the rest of the samples.

The direct U-Pb LA-ICP-MS dating was performed in different laboratories. In the IPGG RAS and GIN SB RAS, the measurements were made using Element XR mass spectrometers with NWR-213 laser ablation systems; the laser beam diameter was 25–30 μm. In the IPGG RAS, isotopic U-Pb age was determined relative to GJ-1 primary (external) standard, and in the GIN SB RAS – relative to Harvard 91500 [Horstwood et al., 2016]. In the IEC SB RAS, U-Pb LA-ICP-MS detrital zircon dating was performed using Agilent 7900 quadrupole mass spectrometer and Analyte Excite laser ablation system; diameter of ablated craters was 35 μm, primary standard – Plešovice zircon [Sláma et al., 2008]. The isotopic age estimates for the secondary (internal) standards obtained in respective laboratories are listed in Table 2 and agree with those obtained by the ID-TIMS method. Isotope ratios based on the IPGG RAS and GIN SB RAS data were calculated using Glitter program [Griffin et al., 2008], and those based on the IEC SB RAS data – in Iolite 4.0 [Paton et al., 2011]. All the age determination errors are at ±2σ level.

Further analysis and graph plotting involved the isotopic age estimates obtained from $^{206}Pb/^{238}U$ ratio for grains younger than 1 Ga and from $^{207}Pb/^{206}Pb$ ratio for older grains. The discordance coefficient was also taken into account depending on zircon age: if it was not older than 1 Ga, there was adopted D_1 value calculated for isotopic age estimate obtained from $^{207}Pb/^{235}U$ and $^{206}Pb/^{238}U$ ratios, or otherwise D_2, calculated based on $^{207}Pb/^{206}Pb$ and $^{206}Pb/^{238}U$ age ratios. The isotopic age values with discordance |D|>10% were rejected. A "soft" filter was chosen due to high sensitivity of statistical tests to relative sample sizes. As compared to the age spectra, obtained through a stricter data filtering, no significant qualitative differences were found. The tables containing all initial LA-ICP-MS detrital zircon dating data are provided in Suppl. 2 on article page online; relationships between Th/U ratios and detrital zircon U-Pb ages are presented in Suppl. 3 on article page online.

Graph plotting and statistical processing of the data were performed using IsoplotR [Vermeesch, 2018] and Dezirteer [Powerman et al., 2021]; the latter was involved in calculating peaks of the age distribution curves. Histograms and Kernel Density Estimation (KDE) curves with a fixed bandwidth "20" were drawn for each sample. Each section plot was normalized so that the areas thereunder were equal. A quantitative comparison of the data was made based on the Kolmogorov – Smirnov (K-S) test. The criterion of Kolmogorov – Smirnov allows identifying the presence of statistically significant difference for a pair of age distributions: if the generated probability is less than the threshold value $p<0.05$, then the source areas of the rocks compared are different (at a $\alpha 95$ confidence level). However, the K-S test can only provide an indirect estimate

Table 2. Data on measurements of the secondary zircon standards

Laboratory	Standard	Isotopic ratio	ID-TIMS ages (Ma)	Source	Ages obtained in the present study (Ma)
IPGG RAS	Harvard 91500	$^{207}Pb/^{206}Pb$ $^{206}Pb/^{238}U$	1066±0.6 1064±0.4	[Horstwood et al., 2016]	1066±5 1065±5
	Plešovice	$^{206}Pb/^{238}U$	337.1±0.4	[Sláma et al., 2008]	336±2
GIN AS RAS	GJ-1	$^{206}Pb/^{238}U$ $^{207}Pb/^{206}Pb$	601.9±0.4 607.7±0.7	[Horstwood et al., 2016]	599±3 586±28
	Plešovice	$^{206}Pb/^{238}U$	337.1±0.4	[Sláma et al., 2008]	338±2
IEC SB RAS	GJ-1	$^{206}Pb/^{238}U$ $^{207}Pb/^{206}Pb$	601.9±0.4 607.7±0.7	[Horstwood et al., 2016]	597±3 619±17
	R33	$^{206}Pb/^{238}U$	419.3±0.4	[Black et al., 2004]	422±3

of the probability of identity among source areas [Guynn, Gehrels, 2010]. This limitation is due to the fact the analysis is only made on the zircon ages which themselves can characterize coeval sources, different in their origin and geographic location. The interpretation should also be done carefully because of sensitivity of the method to the analyzed sample sizes, and inhomogeneity and discreteness of the initial data. The results of the Kolmogorov – Smirnov test were visualized using Multi-Dimensional Scaling (MDS), proposed in [Vermeesch, 2013] as an effective method for analysis of a large number of sets of isotopic ages of detrital zircons. A corresponding diagram reflecting similarity measure between the studied samples was plotted using IsoplotR [Vermeesch, 2018].

3.2. Raman spectroscopy of zircon

Raman spectroscopy of zircon was performed at the Shared Research Facilities of the IEPh RAS [Veselovskiy et al., 2022] using Raman Analyzer EnSpectr R532 for Olympus BX53M optical microscope: laser wave length was 532 nm, power – 30 mW, there was used the 50× objective; the values obtained during five cycles of measurements with a 5 s exposure time were averaged for each grain. An error in the $\nu_3(SiO_4)$ peak location determination is ±1 cm^{-1}. An approximate age of the superimposed thermal events was estimated by the method described in detail in [Resentini et al., 2020]: recalculating the radiation dose so that when fitting a set of points falling within the range of values expected for unannealed grains and a set of points, deviating from that trend to the right part of the plot using least square approximation, the value of the reliability of the approximation R^2 was the maximum.

4. RESULTS AND DISCUSSION

4.1. U-Pb LA-ICP-MS detrital zircon dating

Four stratigraphic levels of the Zhukov ravine reference section were sampled. Sample Zh-56, characterizing the Vokhmian interval of the section, contains zircon grains with a wide range of ages (Fig. 2, a) – from 336 to 3219 Ma. A clearly defined dominant peak of KDE curve with the maximum of 357 Ma is formed by the Paleozoic group (57 %). The isotope-based age estimates for the rest of the grains are rather regularly distributed in the interval of 920–2020 Ma, the Archean grains are single. It is worthy of note that this sample is the least represented and only contains 61 zircon grains with conditional age estimates. The curve of zircon isotopic age distribution for sample Zh-4, selected from the upper Zhukovian horizon, is clearly polymodal (Fig. 2, b). There can be distinguished three clearly defined modes of 363, 1043 and 1635 Ma, as well as three subordinate maximums of 525, 1867 and 2715 Ma. Most of the sample size (85 %) falls within the Proterozoic age interval (938–1988 Ma). Sample Zh-123, also characterizing the Zhukovian interval of the section, resembles the distribution for the Vokhmian part of it (Fig. 2, c). In spite of the fact that the U-Pb ages are distributed in a wide range of 319 to 2695 Ma, almost half of the sample is grouped in a narrow interval with a maximum of 373 Ma. The age of detrital zircon characterizing the lowest of the sampled stratigraphic intervals of the Zhukov ravine section – the upper Nefedovian horizon (sample Zh-11), – varies within the range of 338 to 2747 Ma (Fig. 2, d). About 70 % of the total sample size accounts for the grains with ages of 940–2080 Ma, forming two clearly defined peaks of 1021 and 1781 Ma on KDE curve. The Paleozoic zircon generation forms a clearly defined maximum of 361 Ma. The unrepresentative Late Archean grain population is grouped on the segment with the maximum of 2675 Ma, and three Vendian grains form a small peak of 617 Ma, comparable to similar peaks in the Upper Permian samples Zh-123 and Zh-4. The distribution as a whole reproduces the age spectrum of Zh-4.

The age distributions for all three samples from the Astashikha section (A-4, A-10 и A12D) are almost identical (Fig. 3). Each has the representative Devonian-Carboniferous population with a maximum of about 360 Ma on KDE curve. However, most of the isotopic age estimates (75–80 %) are distributed in the interval of 900–2000 Ma where the curve is bimodal as a whole with the main minimum at a level of about 1300 Ma. A small population of the Vendian – Early Cambrian ages on KDE curve is reliably distinguished only in sample A12D (Fig. 3, a).

Both samples from the Nedubrovo section are unambiguously dominated by the Paleozoic grains whose isotopic age estimates are concentrated in a relatively narrow interval of 290–440 Ma and form a peak with a mode of about 350 Ma on KDE curve (Fig. 4). Against the background of this clearly defined maximum, the rest of the isotopic age estimates, rather regularly distributed within the Proterozoic interval, are poorly defined. Therefore, no significant differences were found between the age spectra obtained for two studied samples, except for an almost two-fold decrease in the share of the Precambrian grains in the upper section: the Proterozoic U-Pb zircon ages make up 34 % of sample H-3 and 16 % of sample H-1.

In sample K-4 (Fig. 5, a) from the Vokhmian interval of the Klykovo section, the most intensive peak on KDE curve with the main maximum of 349 Ma and local maximum of 425 Ma, is formed by the Paleozoic grains making up 44 % of the whole sample. The other part of the sample is comprised of the Archean-Proterozoic grains: in the interval of 900–2000 Ma there are observed several relative maximums, with isolated groups of the Archean grains near an estimate of 2.7 Ga. Worthy of note are also two zircon grains which were found in this sample and whose ages are considered directly similar to the formation time of the rocks studied – 250±3 и 251±3 Ma. Sample K-5 from the Nefedovian horizon of the section differs by almost absolute predominance (87 %) of the Paleozoic zircon grains with a modal value of 349 Ma on the age distribution curve (Fig. 5, b).

Sample Б-3 characterizes the Vokhmian interval of the Balebikha section, which represents a large alluvial channel incision and is similar to K-4 sampling interval of the Klykovo section. However, the detrital zircon age distributions for these two samples are not fully comparable to each other (Fig. 5, a; Fig. 6). Thus, the age spectrum of sample

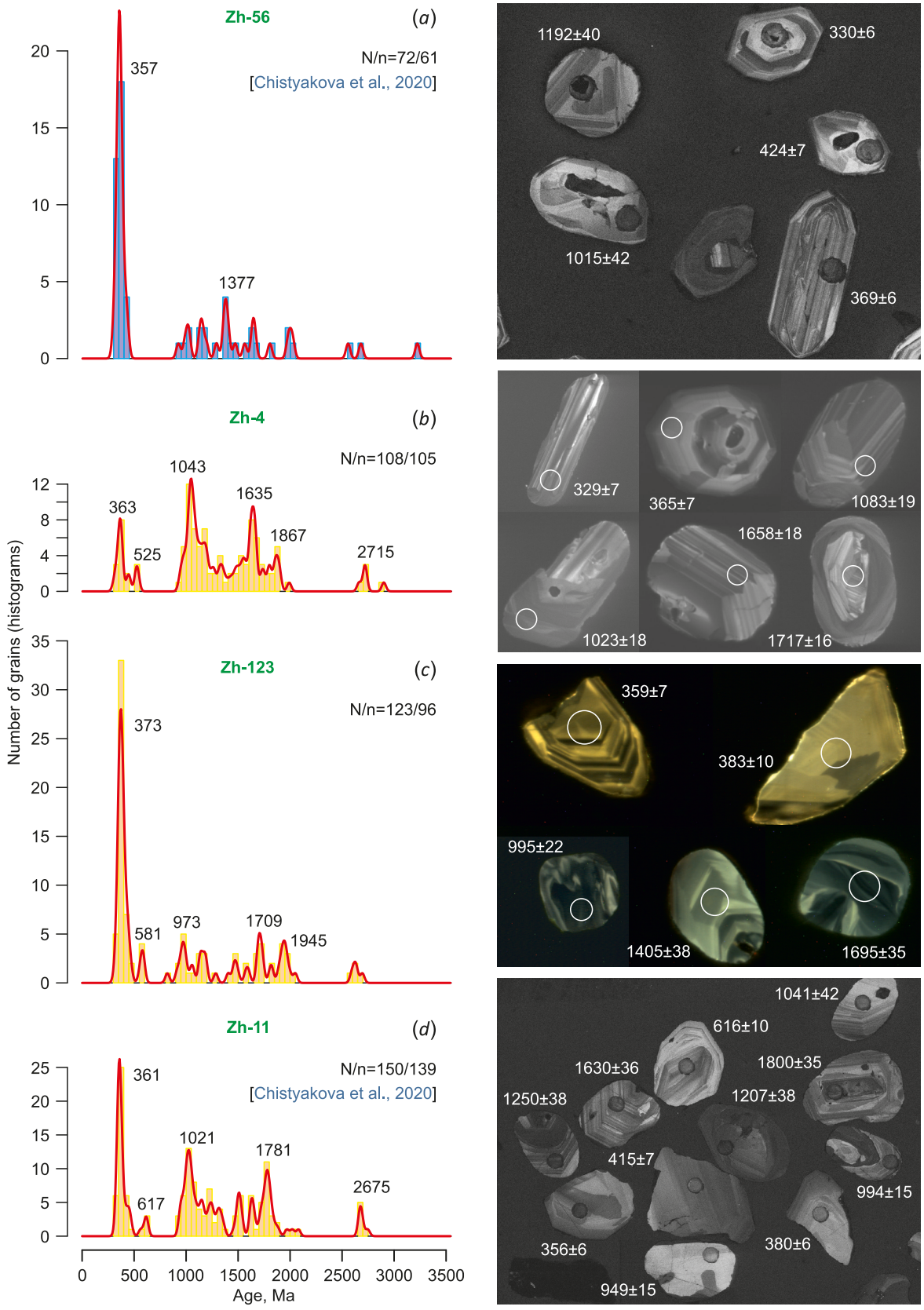

Fig. 2. Normalized detrital zircon U-Pb age distributions (histograms and KDEs) from the Zhukov ravine reference section. On the right are typical CL images of grains from different age populations. N is a total number of grains analyzed; n is a number of grains having discordance <10 %. The numbers mark representative age peaks (Ma).

Б-3 has a distinguished intensive peak for the Paleozoic population with a modal value of 351 Ma, and the age distribution character in the Proterozoic interval is similar to bimodal – two most clearly defined maximums of 997 and 1487 Ma on KDE curve. Besides, unlike the age spectrum for sample К-4, sample К-4 does not have a local maximum close to 400 Ma.

The search for indirect sources of zircon for complexly structured continental units in the central areas of a large platform with a thick cover is a rather specific task [Andersen et al., 2016]. We will provide several versions of interpretation which can complement each other. Judging on the obtained isotopic age estimates, the primary sources of zircon in the studied sections of the Russian basin could be associated with the following crystalline complexes.

1. Devonian and Carboniferous magmatic rocks widespread within the Uralian orogen [Puchkov, 2010; Fershtater, 2013].

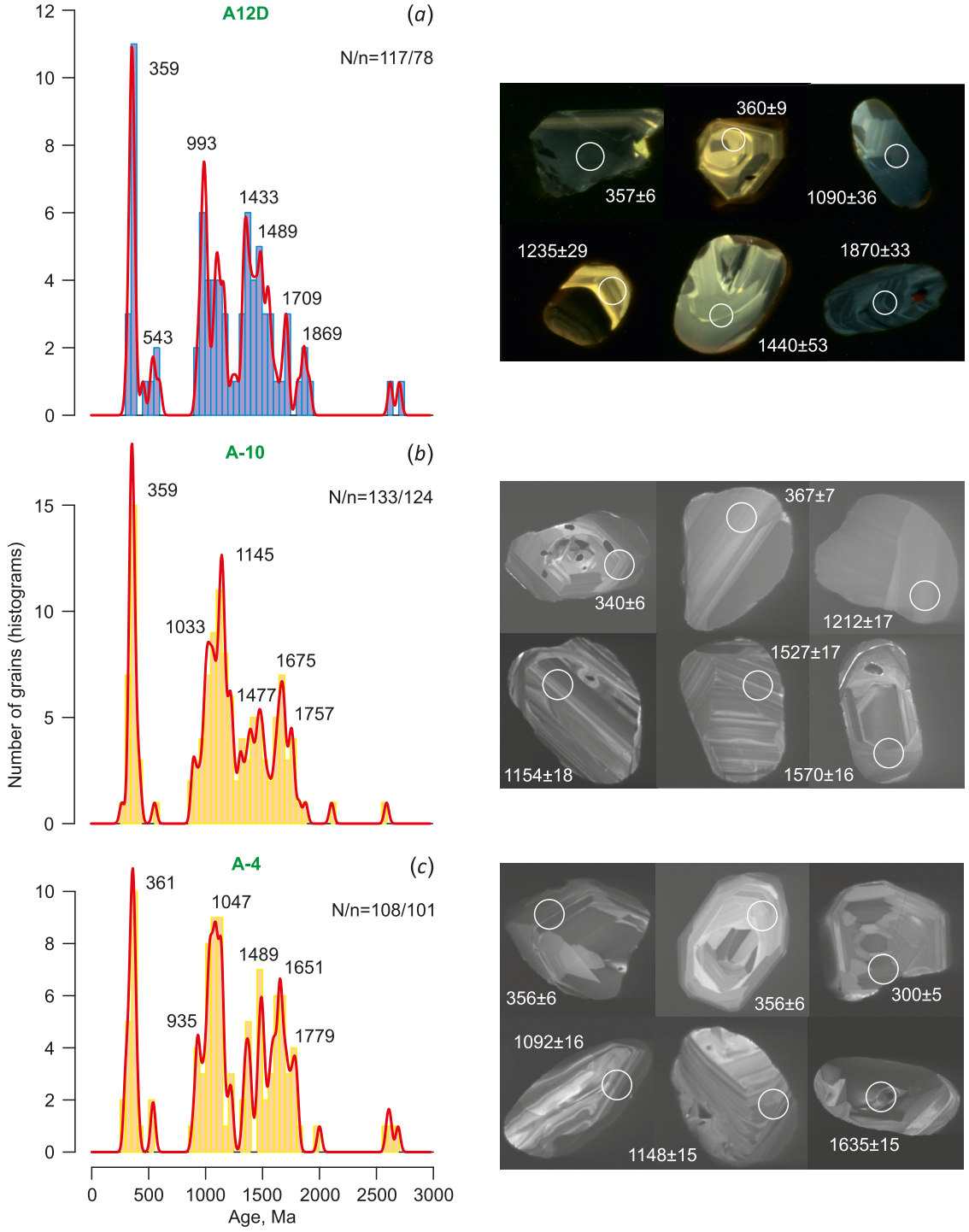

Fig. 3. Normalized detrital zircon U-Pb age distributions (histograms and KDEs) from the Astashikha section. Other designations are the same as in Fig. 2.

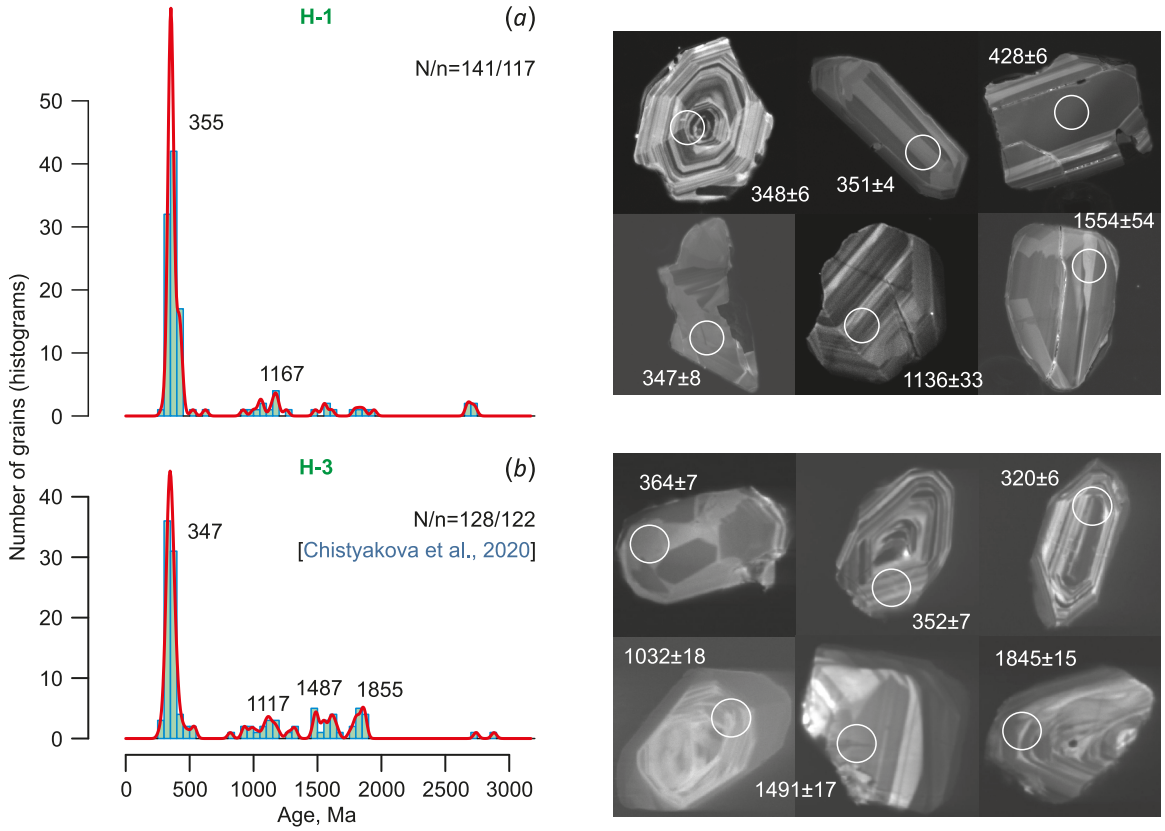

Fig. 4. Normalized detrital zircon U-Pb age distributions (histograms and KDEs) from the Nedubrovo section. Other designations are the same as in Fig. 2.

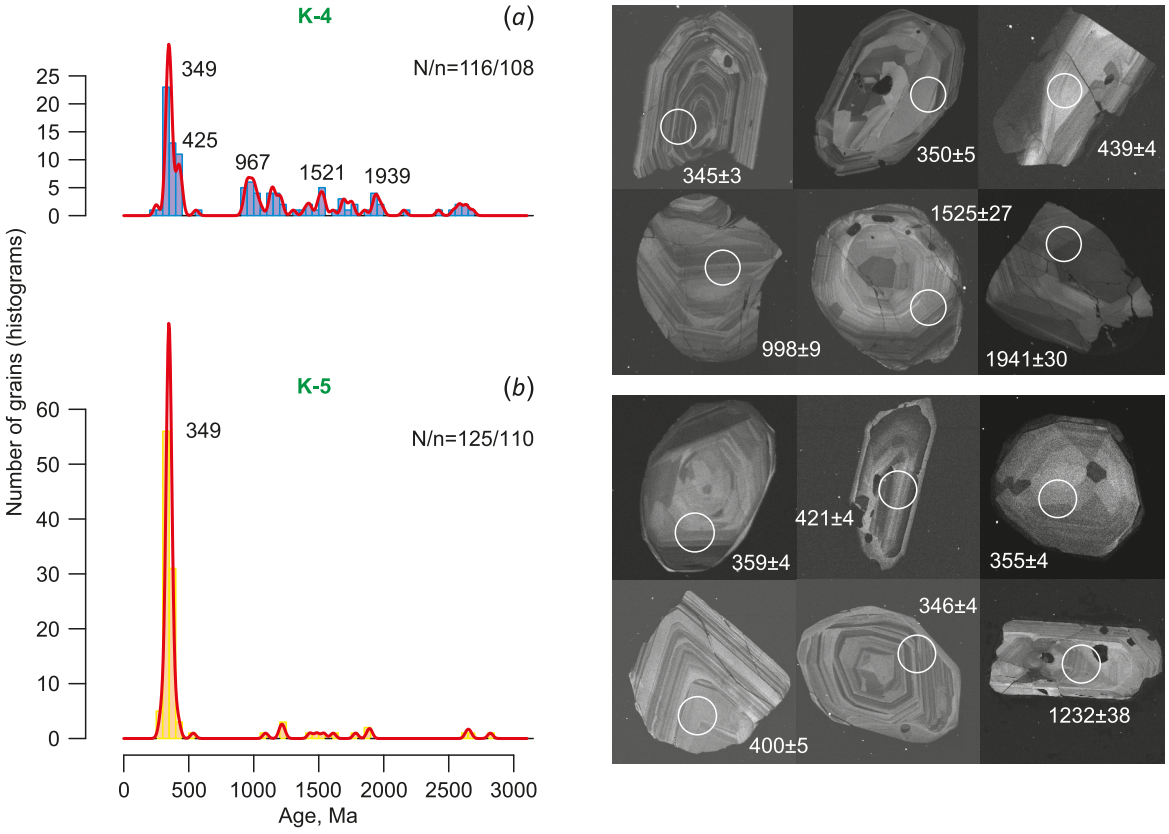

Fig. 5. Normalized detrital zircon U-Pb age distributions (histograms and KDEs) from the Klykovo section. Other designations are the same as in Fig. 2.

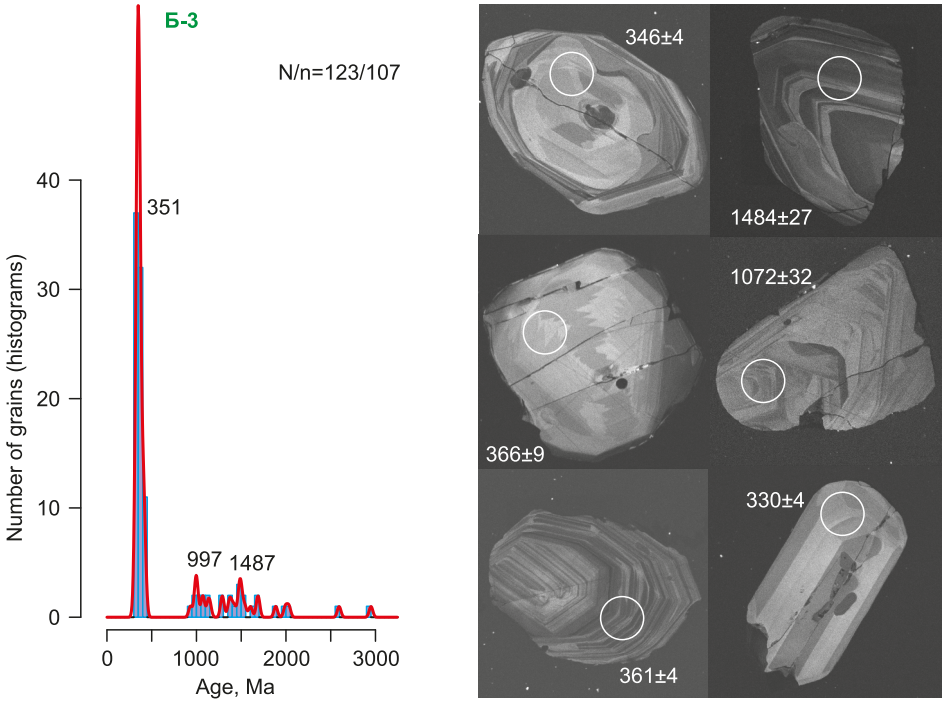

Fig. 6. Detrital zircon U-Pb age distribution (histogram and KDE) from the Balebikha section. Other designations are the same as in Fig. 2.

2. Complexes related to the processes of initiation of the Timan (Protouralian) foldbelt in the interval 530–750 Ma [Puchkov, 2010; Soboleva et al., 2012; Kuznetsov et al., 2014a].

3. The Sveconorwegian [Bingen et al., 2021; Mints, 2017] and Svecofennian [Daly et al., 2006] exposures of crystalline rocks which are characterized by zircon ages of about 1.0 and 1.6–1.8 Ga, respectively. However, the Proterozoic zircon-bearing rocks are also known for the complexes making up the basement of the Timan-Pechora region and locally exposed near the Timan Ridge [Pystin et al., 2020, and references therein]. Nevertheless, there can also exist the third way the Proterozoic zircon entered the central parts of the East European Platform: the studies of the Vendian-Paleozoic terrigenous complexes of the South Ural [Kuznetsov et al., 2014b] showed the presence of detrital zircon grains whose age distributions therein are similar to those known for Fennoscandia. The remoteness (more than 2000 km) of the Svecofennian and Sveconorwegian domains allowed the authors to suggest the presence of extra-Baltic sources with similar age characteristics. Thus, there remains an identification ambiguity for distributive province with the "Fennoscandian" signal, revealed as a result of the heavy mineral analysis [Lozovsky, Esaulova, 1998].

4. Late Archean complexes of the Karelia-Kola and/or Volga-Ural regions [Daly et al., 2006].

5. Other local exposures of the East European Platform Archean-Proterozoic basement.

Direct source areas in formation of the Permian to Triassic rocks of the Russian Platform could obviously be relatively older sedimentary rocks formed earlier as a result of erosion of the described crystalline complexes. Among other things, we cannot exclude a rather high degree of zircon recycling directly across the studied Permian-Triassic continental units.

Thus, the present paper characterizes distributive areas in terms of "provenance-signals" – representative sets of zircon age values, related to the most typical and widespread magmatic, metamorphic and terrigenous complexes of certain regions, and corresponding to their different developmental stages. However, taking into account high retained variability of interpretation of the Precambrian zircon grains, we propose to consider the revealed provenance-signals, first of all, in terms of their contrasting age characteristics and distinguish the Vendian-Paleozoic and Paleo-Mesoproterozoic signals. It should be noted that due to the correspondence between the main KDE maximums and known global episodes of tectono-magmatic activation [Pastor-Galán et al., 2019], an extremely wide interpretation of potential sources of zircon is allowed to be based solely on the U-Pb ages.

Fig. 7 shows a version of stratigraphic correlation for five studied Permian-Triassic sections based on biostratigraphic, magnetostratigraphic and isotopic-geochemical data. The sections are represented by red-colored sandy-clay rocks of the Nefedovian, Zhukovian and Vokhmian horizons. However, at present it is not possible to obtain a reliable localization of the Permian-Triassic boundary (the boundary between the Upper Vyatkian Substage and the Induan Stage, respectively) in the considered stratigraphic successions of the Russian Platform. Nevertheless, in accordance with the isotopic-geochemical data, the Permian-Triassic boundary is located within the Lower Vokhmian Subhorizon.

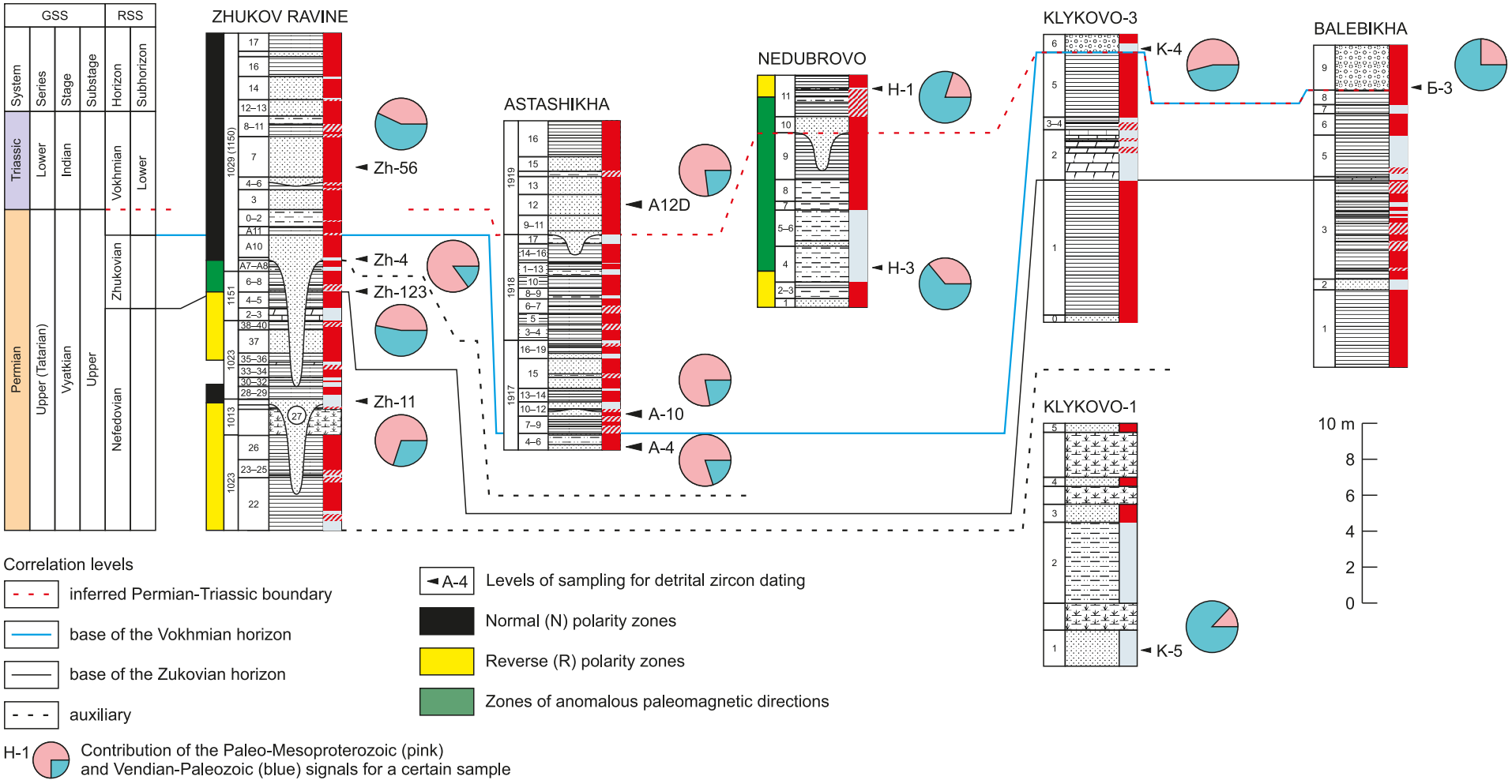

Fig. 7. The stratigraphic correlation of the studied Permian-Triassic boundary sections, compiled by V.K. Golubev using the original data and the data published in [Arefiev et al., 2016a, 2016b; Fetisova et al., 2018, 2022].

Complex analysis of the U-Pb ages of detrital zircons from the central areas of the East European Platform revealed the following regularities (Fig. 8). Generally there are two types of age spectra to be distinguished:

(1) the sample provides a fairly even representation of the Archean-Proterozoic and Paleozoic (50–80 % of the entire sample) populations, though a clearly defined dominant peak of KDE curve falls within the interval 350–370 Ma (for example, sample Zh-56, see Fig. 2, a);

(2) most of the sample (70–85 %) is represented by the population of the Archean-Proterozoic grains which usually splits into two subpopulations, and the Paleozoic population of grains is subordinate thereto (for example, sample Zh-4, see Fig, 2, b).

The detrital zircon age distribution (Fig. 8), obtained for the Lower Nefedovian stratigraphic level (sample К5) is related to spectra of the first type (no less than 50 % contribution from the Vendian-Paleozoic provenance-signal). Upward the section, in the Upper Nefedovian layers (sample Zh-11), there occurs the age spectrum of the second type – with the dominance of the Paleo-Mesoproterozoic provenance-signal (70–85 %). Just ~7 m further upwards, in the Lower Zhukovian stratigraphic interval (Zh123 sampling level), there is observed a reorganization of distributive areas in favor of the dominant Vendian-Paleozoic signal. However, no further than the Upper Zhukovian part of the section, within the boundaries of the stratigraphic interval combining samples Zh-4 and A-4, there is another occurrence of reliable correlation in detrital zircon age spectra of the second type with a clear dominance of the Paleo-Mesoproterozoic signal. A regular alternation of two types of detrital zircon age distributions continues even further. The age spectra of the first type were obtained for the Vokhmian intervals of the Zhukov ravine and Klykovo and Balebikha sections (samples Zh56, К-4, Б3). However, the Vokhmian level of the Astashikha section (samples A-10 and A12D) is characterized by no less than 70–85 % share of the Paleo-Mesoproterozoic provenance-signal. Therefore, the stratigraphic analogs of the Vokhmian deposits of the Astashikha section in the Zhukov ravine section are (1) located in the lower Vokhmian horizon below Zh-56 sampling level or (2) entirely absent (stratigraphic break).

If the age distributions of detrital zircons from the Zhukov ravine section are considered as reference to corresponding stratigraphic levels within the Moscow basin, then the stratigraphic scheme could also be clarified as follows (see Fig. 7). The new paleomagnetic [Fetisova et al., 2022] and geochronological data imply that that the rocks of the Nedubrovo section correlate with an anomalous paleomagnetic recording interval in the lower Zhukovian horizon of the Zhukov ravine reference section characterized by sample Zh-123 (see Fig. 7). However, the upper bound of the compared interval is Zh-4 sampling level which reflects the reorganization of distributive areas in favor of

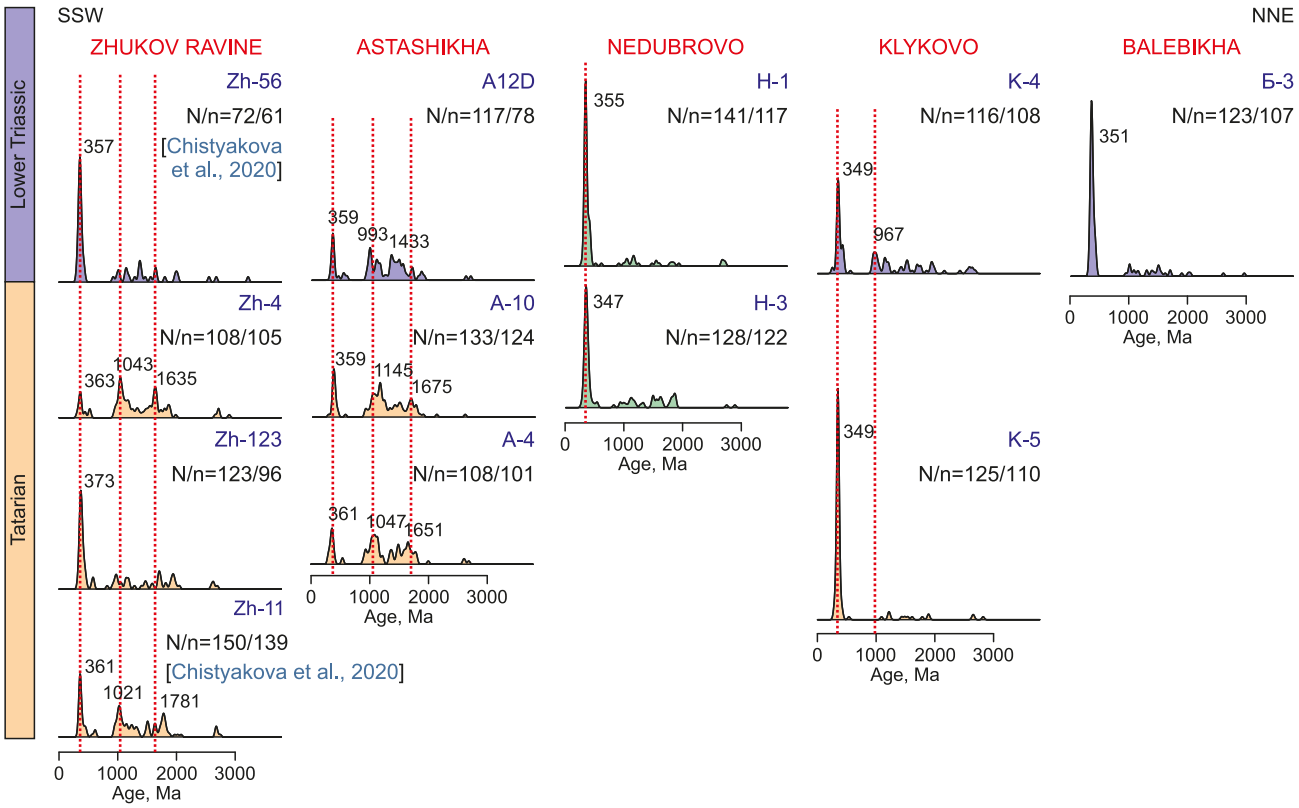

Fig. 8. Results of U-Pb LA-ICP-MS dating of detrital zircon from the Permian-Triassic boundary sections of the eastern part of the Moscow basin (normalized KDEs).
N – a total number of grains analyzed; n – a number of grains having discordance <10 %. The numbers mark representative age peaks (Ma). The dotted lines are drawn across the main age peaks of KDE curves.

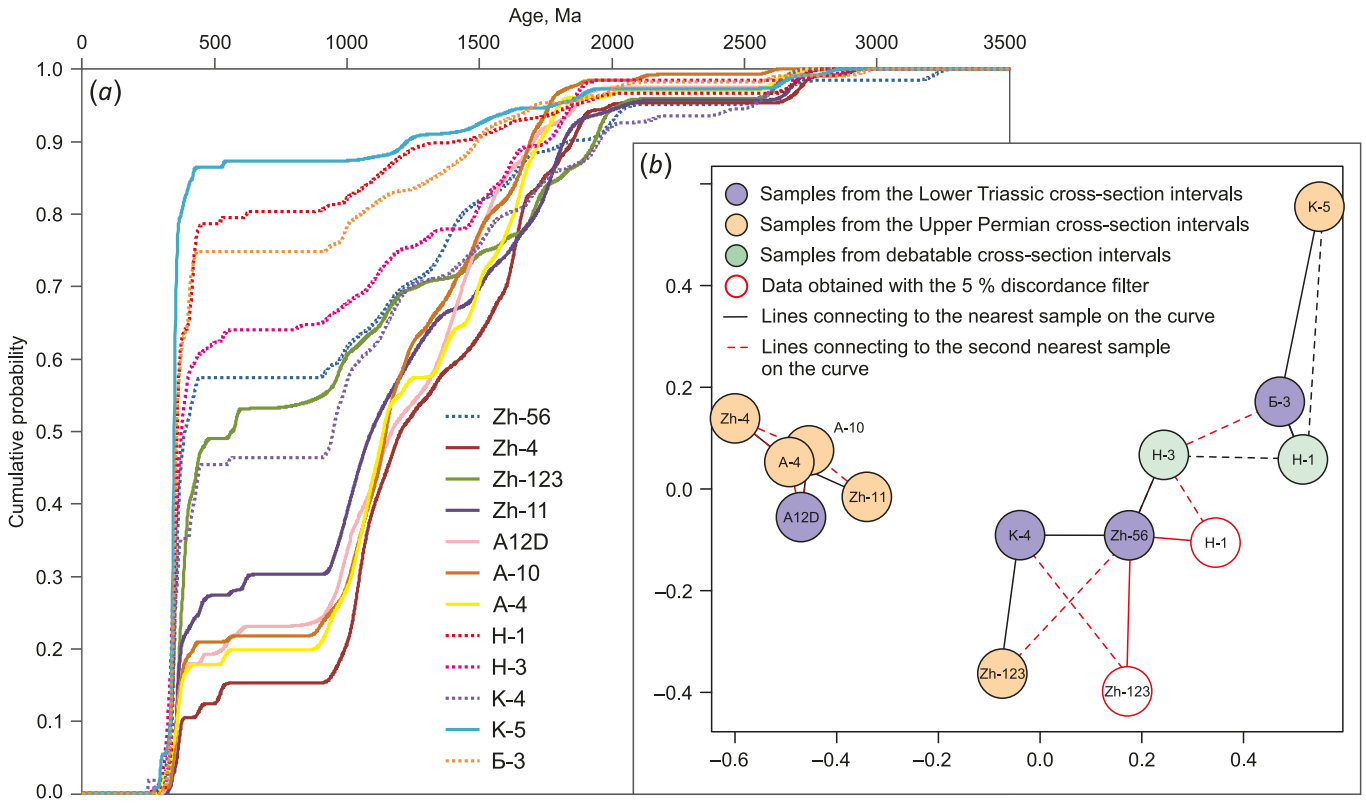

Fig. 9. Compared cumulative curves for age spectra of zircon from the studied sections (*a*) and Kolmogorov – Smirnov-based Multi-dimensional scaling (MDS) plot reflecting the degree of difference/similarity between the obtained zircon age distributions (*b*).

Table 3. Results of the Kolmogorov – Smirnov test (*p* values calculated taking into account errors in isotopic age determination)

Section	Zhukov ravine				Astashikha			Nedubrovo		Klykovo		Balebikha
Interval												
Sample	Zh-56	Zh-4	Zh-123	Zh-11	A12D	A-10	A-4	H-1	H-3	K-4	K-5	Б-3
Zh-56		0.000	0.065	0.000	0.000	0.000	0.000	0.029	0.677	0.254	0.000	0.134
Zh-4			0.000	0.039	0.228	0.184	0.888	0.000	0.000	0.000	0.000	0.000
Zh-123				0.002	0.001	0.000	0.000	0.000	0.001	0.119	0.000	0.000
Zh-11					0.591	0.331	0.480	0.000	0.000	0.021	0.000	0.000
A12D						0.884	0.903	0.000	0.000	0.003	0.000	0.000
A-10							0.852	0.000	0.000	0.000	0.000	0.000
A-4								0.000	0.000	0.000	0.000	0.000
H-1									0.048	0.000	0.002	0.988
H-3										0.007	0.000	0.176
K-4											0.000	0.000
K-5												0.009
Б-3												

Legend:

Lower Triassic interval of the section

Upper Permian interval of the section

Debatable interval

0.065 0.029 Parameter *p*; if $p<0.050$, then sources of detrital zircons are different (at 95% confidence level)

the dominant Paleo-Mesoproterozoic provenance-signal. Thus, we are inclined to reconsider the conclusions drawn in [Chistyakova et al., 2020] and, according to publicly available dataset, to relate the entire Nedubrovo section to the Early Zhukovian age. Nevertheless, the remoteness of the Nedubrovo section from the Zhukov ravine reference section does not allow using new isotopic-geochronological data for convincing justification of stratigraphic position of the Nedubrovo layers. In this connection, when compiling the scheme of evolution of distributive areas, we considered the models based on two versions of stratigraphic position of samples H-3 and H-1: Vokhmian and Lower Zhukovian.

Highly contrasting age distributions of detrital zircons from the Permian-Triassic complexes of the Moscow syneclise are illustrated by the graph of difference between cumulative curves (Fig. 9, a), which lies in the basis of statistical comparison on the criterion of Kolmogorov – Smirnov. The results of the Kolmogorov – Smirnov test (Table 3) are visualized in multidimensional scaling (MDS) plot (Fig. 9, b): the degree of similarity between the samples therein reflects the degree of their similarity on the criterion of Kolmogorov – Smirnov. During the work the results obtained with the 10 % discordance filter (used in all graphics and value calculations in Table 3) were compared to those obtained with the 5 % discordance filter: both versions were kept in case of a significant difference between the positions of the same sample on the MDS plot.

Samples on the MDS plot form two clusters, thus indicating a principal difference between the debris source areas for the rocks therefrom. It is worthy of note that samples Zh-4, A-4, A-10, A12D and Zh-11 form a more compact cluster, i.e., are more similar in their source areas.

4.2. Raman spectroscopy

Raman spectroscopy method was used to study eleven samples characterizing the Moscow syneclise (Suppl. 4 on article page online). All plots of the relationship between

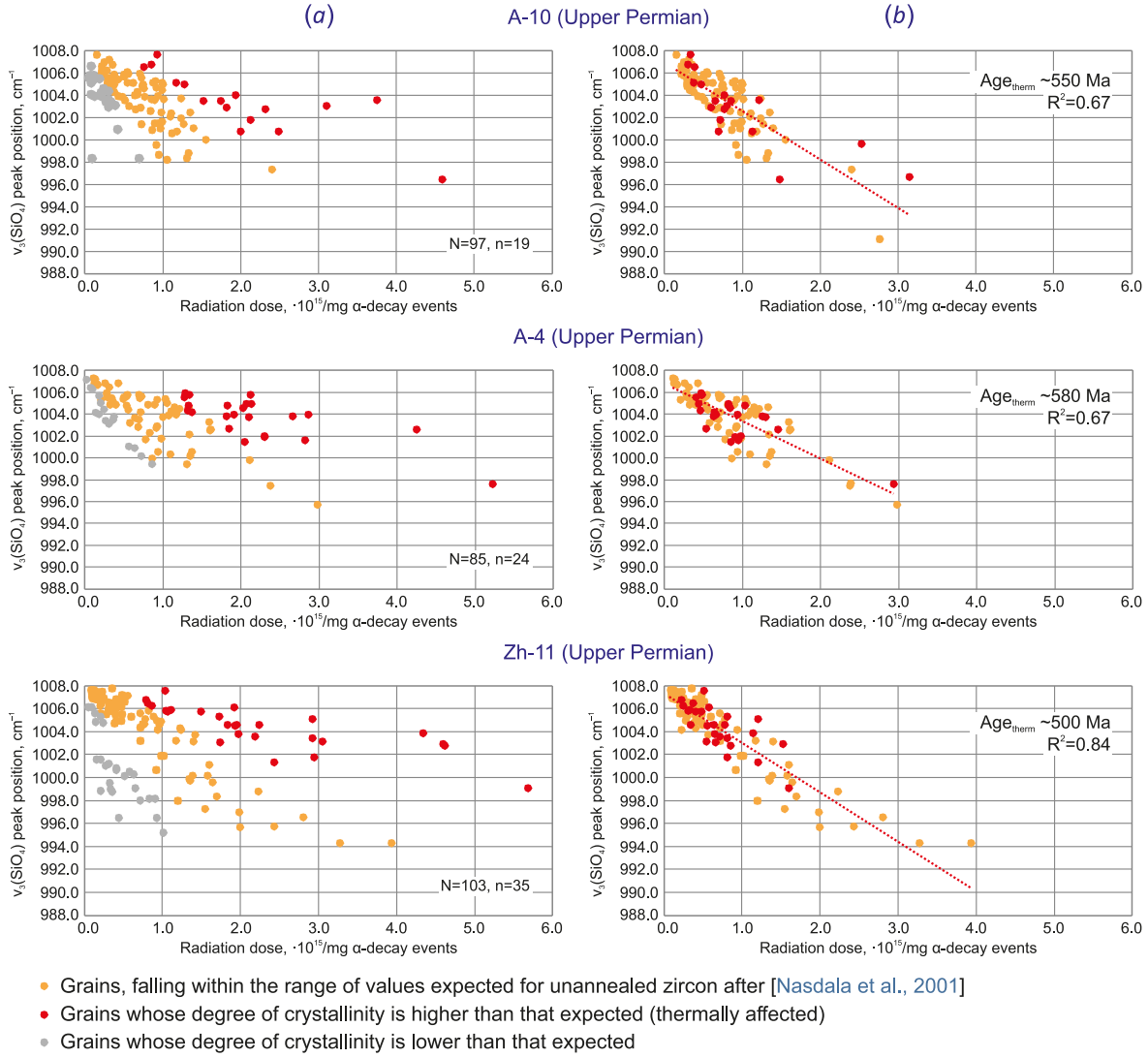

Fig. 10. Relationship between $\nu_3(SiO_4)$ Raman peak position and accumulated alfa-radiation dose.
(*a*) – obtained initially, (*b*) – obtained after iterative estimation of the thermal event age. R^2 – linear approximation confidence value. $Age_{thermal}$ – the proposed age of the thermal event. N – a total number of grains analyzed; n – a number of annealed grains.

the $\nu_3(SiO_4)$ peak position and calculated alfa-radiation dose (Fig. 10; Suppl. 4) show the clusters of points deviating significantly from the empirical trend obtained for zircon which was not thermally annealed [Nasdala et al., 2001]. The points can be shifted both to the right and to the left from this trend. In the first case (red dots in Fig. 10, a), the shift is partially attributed to thermal restoration of the crystalline structure of zircon. The observed increase in the degree of crystallinity (the $\nu_3(SiO_4)$ Raman peak shift is much less than that expected for the corresponding alfa dose – gray dots in Fig. 10, a), probably reflects a high degree of hydrothermal alteration of the rocks [Kaulina et al., 2017]. Further calculations were made with no regard to analyses with underestimations of the degree of crystallinity.

Statistically significant (20–30 %) amount of thermally annealed grains was recorded in three samples from the Upper Permian interval: Zh-11 (Zhukov ravine section), and A-10 and A-4 (Astashikha section). Based on these samples, age estimates were made of thermal events (Fig. 10, b). It is supposed that the ages corresponding to thermal events were about 500, 550 and 580 Ma for samples Zh-11, A-10 and A-4, respectively. Taking into account a high error in the results, we are inclined to consider the obtained ages as part of the single Vendian-Cambrian thermal event.

Complex analysis of the results for Raman spectroscopy and U-Pb LA-ICP-MS dating of detrital zircon (Fig. 11) showed that thermally affected grains were those with ages ranging between 900 and 3200 Ma. There is relatively equal proportion of zircon from all groups forming significant peaks on the age distribution curve in the range mentioned. A wide range of ages of thermally annealed grains may imply that the thermal event occurred in some intermediate sedimentary basin. The Vendian-Cambrian age of the supposed thermal event allows us to correlate it with tectonomagmatic processes related to the Timan (Proto-uralian) folded structure whose relics are found within the present-day Uralian orogen [Puchkov, 2010]. Therefore, the described intermediate basin should have been located

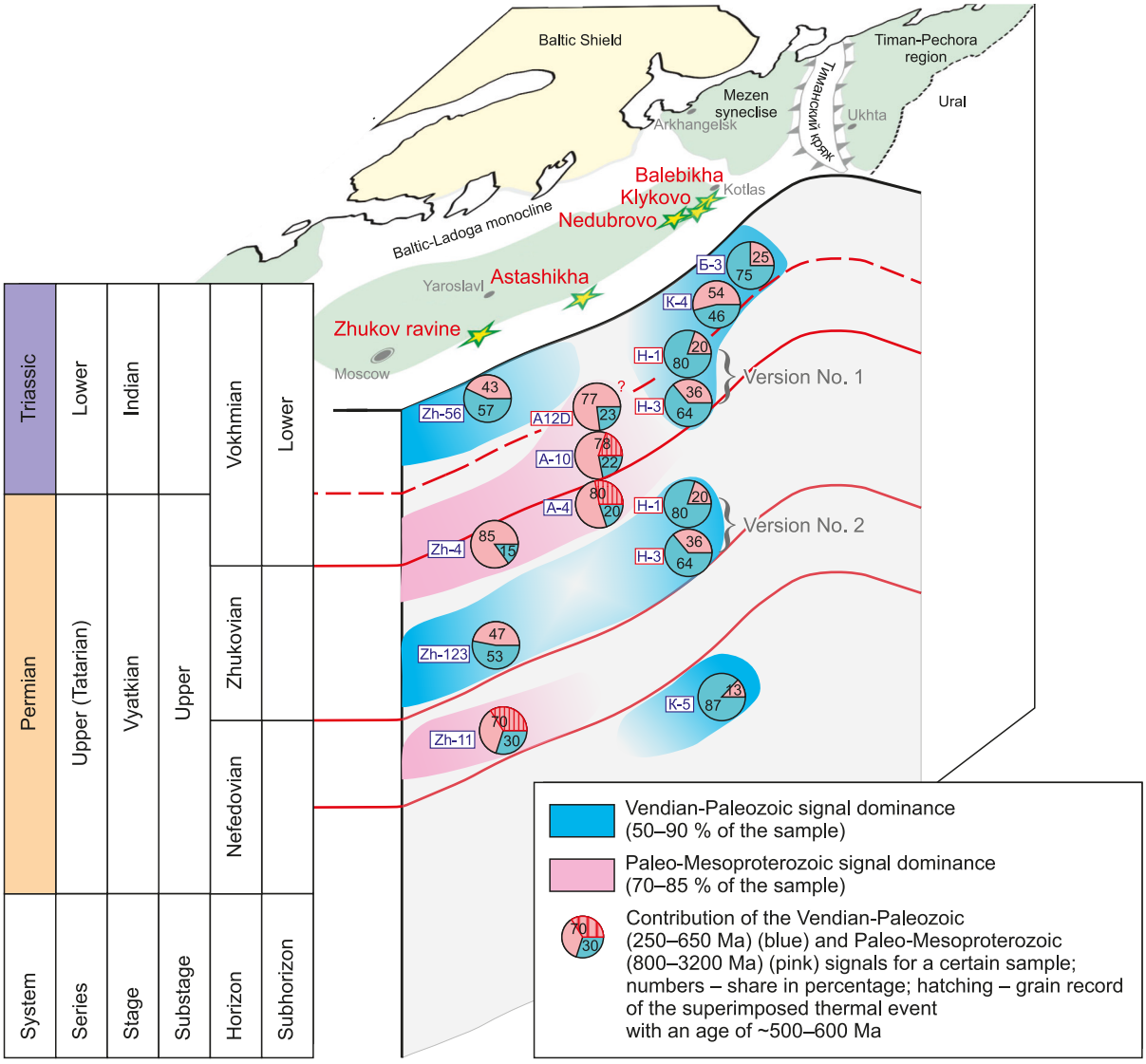

Fig. 11. Evolution of provenance of the Permian-Triassic detritus from the eastern part of the Moscow basin. The scheme represents two versions of stratigraphic position of the Nedubrovo section.

near the eastern or, in terms of modern coordinates, northeastern margin of the East European Platform.

5. CONCLUSION

Analysis has been made on 1400 zircon grains extracted from 12 samples which were taken from 5 sections of Permian-Triassic sequences of the eastern part of the Moscow basin. From the Permian-Triassic terrigenous complex of the East European Platform there were for the first time obtained representative isotopic-geochronological data, used for the reconstruction of source areas of the Moscow basin at the Paleozoic-Mesozoic boundary. It is shown that in a number of cases the results of detrital zircon dating can serve as a publicly available data source to clarify the schemes of intrabasin correlation and sequence stratigraphic division of the formations considered.

The main conclusions drawn herein are the following:

1. The results of U-Pb LA-ICP-MS detrital zircon dating confirm the earlier heavy-mineral-analysis-based suggestion [Arefiev et al., 2016b; Strok, Trofimova, 1976] that the Permian-to-Triassic sedimentary complexes in the central East European Platform formed under competitive conditions among two main source areas.

2. These competing source areas are characterized by two contrast provenance-signals – Vendian-Paleozoic and Paleo-Mesoproterozoic.

3. During the Late Vyatkian, the reorganization of source areas of the Moscow basin occurred at least twice (Fig. 11). There is an observed alternation between mode of domination of source areas with the Paleo-Mesoproterozoic signal and debatable geological position (75–80 % of the sample), and mode of intensification of detritus removal with the Vendian-Paleozoic provenance-signal into the Moscow basin due to erosion of the complexes of the Uralides (50–75 % of the sample). Another similar reconstruction occurred in the Vokhmian and, probably, reflects global changes directly at the Permian-Triassic boundary.

4. In the Late Permian, one of the source areas of the Moscow basin was a terrigenous complex whose rocks experienced a relatively low-temperature superimposed impact in the Vendian-Cambrian time (~500–600 Ma) due to tectonomagmatic processes of the initiation and development of the Timanides-Protouralides.

6. ACKNOWLEDGEMENTS

The authors express their sincere gratitude to V.P. Kovach, E.V. Adamskaya, T.I. Golovanova and M.N. Savelyeva for analytical studies, and to K.G. Erofeeva, N.B. Kuznetsov, T.V. Romanyuk and V.I. Powerman for the comments and constructive criticism.

7. CONTRIBUTION OF THE AUTHORS

All authors made an equivalent contribution to this article, read and approved the final manuscript.

8. DISCLOSURE

The authors declare that they have no conflicts of interest relevant to this manuscript.

9. REFERENCES

Andersen T., Kristoffersen M., Elburg M.A., 2016. How Far Can We Trust Provenance and Crustal Evolution Information from Detrital Zircons? A South African Case Study. Gondwana Research 34, 129–148. https://doi.org/10.1016/j.gr.2016.03.003.

Arefiev M.P., 2016a. Ideal Cyclite of a Compensated Trough and the Cyclicity Nature of the Permian-Triassic Red Beds of the East European Platform. In: Sedimentary Complexes of the Urals and Adjacent Regions and Their Mineralogy. Proceedings of XI Ural Lithological Meeting (October 17–19, 2016). IGG UB RAS Publishing House, Ekaterinburg, p. 22–24 (in Russian) [Арефьев М.П. Идеальный циклит компенсированного прогиба и природа цикличности красноцветной пермо-триасовой формации Восточно-Европейской платформы // Осадочные комплексы Урала и прилежащих регионов и их минерагения: Материалы XI Уральского литологического совещания (17–19 октября 2016 г.). Екатеринбург: Изд-во ИГГ УрО РАН, 2016. С. 22–24].

Arefiev M.P., 2016b. Isotope-Geochemical Characteristics ($\delta^{13}C$, $\delta^{18}O$) of the Continental Permian-Triassic Sequences of the East European Platform: Paleogeographic Restructuring in the Light of Global Climate Trends. In: Unique Lithological Objects Through the Prism of Their Diversity. Proceedings of 2nd School of Students, Graduate Students and Young Scientists in Lithology (October 21–24, 2016). IGG UB RAS Publishing House, Ekaterinburg, p. 12–18 (in Russian) [Арефьев М.П. Изотопно-геохимическая характеристика ($\delta^{13}C$, $\delta^{18}O$) континентальных пермо-триасовых отложений Восточно-Европейской платформы: палеогеографическая перестройка в свете глобальных климатических трендов // Уникальные литологические объекты через призму их разнообразия: Материалы 2-й Всероссийской школы студентов, аспирантов и молодых ученых по литологии (21–24 октября 2016 г.). Екатеринбург: Изд-во ИГГ УрО РАН, 2016. С. 12–18].

Arefiev M.P., Golubev V.K., Balabanov Yu.P., Karasev E.V., Minikh A.V., Minikh M.G., Molostovskaya I.I., Yaroshenko O.P., Zhokina-Naumcheva M.A., 2015. Type and Reference Sections of the Permian–Triassic Continental Sequences of the East European Platform: Main Isotope, Magnetic, and Biotic Events. Proceedings of XVIII International Congress on Carboniferous and Permian. Sukhona and Severnaya Dvina Rivers Field Trip (August 4–10, 2015). PIN RAS, Moscow, 104 p.

Arefiev M.P., Golubev V.K., Karasev E.V., Kuleshov V.N., Pokrovsky B.G., Shkursky B.B., Yaroshenko O.P., Grigorieva A.V., 2016a. Paleontology, Sedimentology and Geochemistry of Terminal Permian in Northeastern Part of Moscow Syneclise. 2. Lower Stream of Yug River. Bulletin of Moscow Society of Naturalists. Geological Series 91 (2–3), 47–62 (in Russian) [Арефьев М.П., Голубев В.К., Карасев Е.В., Кулешов В.Н., Покровский Б.Г., Шкурский Б.Б., Ярошенко О.П., Григорьева А.В. Комплексная палеонтологическая, седиментологическая и геохимическая характеристика терминальных отложений пермской системы северо-восточного борта Московской синеклизы. Статья 2.

Нижнее течение р. Юг // Бюллетень МОИП. Отдел геологический. 2016. Т. 91. Вып. 2–3. С. 47–63].

Arefiev M.P., Golubev V.K., Kuleshov V.N., Kukhtinov D.A., Minikh A.V., Pokrovsky B.G., Silantiev V.V., Urazaeva M.N., Shkursky B.B., Yaroshenko O.P., Grigorieva A.V., Naumcheva M.A., 2016b. Paleontology, Sedimentology and Geochemistry of the Terminal Permian in Northeastern Part of Moscow Syneclise. 1. Malaya Severnaya Dvina River Basin. Bulletin of Moscow Society of Naturalists. Geological Series 91 (1), 24–49 (in Russian) [Арефьев М.П., Голубев В.К., Карасев Е.В., Кулешов В.Н., Покровский Б.Г., Шкурский Б.Б., Ярошенко О.П., Григорьева А.В. Комплексная палеонтологическая, седиментологическая и геохимическая характеристика терминальных отложений пермской системы северо-восточного борта Московской синеклизы. Статья 1. Бассейн реки Малая Северная Двина // Бюллетень МОИП. Отдел геологический. 2016. Т. 91. № 1. С. 24–49].

Arefiev M.P., Golubev V.K., Naumcheva M.A., 2017. Preliminary Correlation of the Permian and Triassic Boundary Rocks in the Yug and Vetluga Basins. In: A.S. Alekseev (Ed.), Paleostrat-2017. Annual Meeting (Scientific Conference) of the Paleontology Section of the Moscow Society of Naturalists and the Moscow Branch of the Paleontological Society at the Russian Academy of Sciences (January 30 – February 1, 2017). Abstracts. PIN RAS, Moscow, p. 6–7 (in Russian) [Арефьев М.П., Голубев В.К., Наумчева М.А. Предварительная корреляция пограничных отложений перми и триаса в бассейнах Юга и Ветлуги // Палеострат-2017. Годичное собрание (научная конференция) секции палеонтологии МОИП и Московского отделения Палеонтологического общества при РАН (30 января – 1 февраля 2017 г.): Тезисы докладов / Ред. А.С. Алексеев. М.: Палеонтологический институт им. А.А. Борисяка РАН, 2017. С. 6–7].

Bingen B., Viola G., Möller C., Vander Auwera J., Laurent A., Yi K., 2021. The Sveconorwegian Orogeny. Gondwana Research 90, 273–313. https://doi.org/10.1016/j.gr.2020.10.014.

Black L.P., Kamo S.L., Allen C.M., Davis D.W., Aleinikoff J.N., Valley J.W., Mundil R., Campbell I.H., Korsch R.J., Williams I.S., Foudoulis C., 2004. Improved $^{206}Pb/^{238}U$ Microprobe Geochronology by the Monitoring of a Trace Element Related Matrix Effect; SHRIMP, ID TIMS, ELA ICP MS and Oxygen Isotope Documentation for a Series of Zircon Standards. Chemical Geology 205 (1–2), 115–140. https://doi.org/10.1016/j.chemgeo.2004.01.003.

Chistyakova A.V., Veselovskiy R.V., Semenova D.V., Kovach V.P., Adamskaya E.V., Fetisova A.M., 2020. Stratigraphic Correlation of Permian–Triassic Red Beds, Moscow Basin, East European Platform: First Detrital Zircon U-Pb Dating Results. Doklady Earth Sciences 492, 306–310. https://doi.org/10.1134/S1028334X20050062.

Daly J.S., Balagansky V.V., Timmerman M.J., Whitehouse M.J., 2006. The Lapland-Kola Orogen: Palaeoproterozoic Collision and Accretion of the Northern Fennoscandian Lithosphere. Geological Society of London, Memoirs 32, 579–598. https://doi.org/10.1144/GSL.MEM.2006.032.01.35.

Fershtater G.B., 2013. Paleozoic Intrusive Magmatism of the Middle and South Urals. Publishing House of the Ural Branch of RAS, Ekaterinburg, 368 p. (in Russian) [Ферштатер Г.Б. Палеозойский интрузивный магматизм Среднего и Южного Урала. Екатеринбург: Изд-во УРО РАН, 2013. 368 с.].

Fetisova A.M., Balabanov Yu.P., Veselovsky R.V., Mamontov D.A., 2018. Anomalous Magnetization of the Permian–Triassic Nedubrovo Red Beds, Moscow Basin. Vestnik of Saint Petersburg University. Earth Sciences 63 (4), 544–560 (in Russian) [Фетисова А.М., Балабанов Ю.П., Веселовский Р.В., Мамонтов Д.А. Аномальная намагниченность красноцветов недубровской пачки пограничных пермо-триасовых отложений Русской плиты // Вестник СПбГУ. Науки о Земле. 2018. Т. 63. № 4. С. 544–560]. https://doi.org/10.21638/spbu07.2018.409.

Fetisova A.M., Golubev V.K., Veselovskiy R.V., Balabanov Yu.P., 2022. Paleomagnetism and Magnetostratigraphy of Permian–Triassic Reference Sections in the Central Russian Plate: Zhukov Ravine, Slukino, and Okskiy Siyezd. Russian Geology and Geophysics 63 (10), 1162–1176. https://doi.org/10.2113/RGG20214336.

Golubev V.K., 2016. Regional Stratigraphic Scheme of the Permian System of the East European Platform: Current State and Problems. In: State of the Stratigraphic Base of the Center and Southeast of the East European Platform. Proceedings of Meeting (November 23–25, 2015). VNIGRI, Moscow, p. 72–79 (in Russian) [Голубев В.К. Региональная стратиграфическая схема пермской системы Восточно-Европейской платформы: современное состояние и проблемы // Состояние стратиграфической базы центра и юго-востока Восточно-Европейской платформы: Материалы совещания (23–25 ноября 2015 г.). М.: ВНИГРИ, 2016. С. 72–79].

Golubev V.K., 2019. Permian-Triassic Boundary Stratigraphy of the East European Platform. The State of the Art: No Evidence for a Major Temporal Hiatus. Permophiles: Newsletter of Subcommission on Permian Stratigraphy 67, p. 33–36.

Golubev V.K., Minikh A.V., Balabanov Yu.P., Kukhtinov D.A., Sennikov A.G., Minikh M.G., 2012. Reference Section of the Permian and Triassic in the Zhukov Ravine near the City of Gorokhovets, Vladimir Region. Bulletin of the Regional Interdepartmental Stratigraphic Commission for the Center and South of the Russian Platform 5, 49–82 (in Russian) [Голубев В.К., Миних А.В., Балабанов Ю.П., Кухтинов Д.А., Сенников А.Г., Миних М.Г. Опорный разрез перми и триаса в Жуковом овраге у г. Гороховец, Владимирская область // Бюллетень Региональной межведомственной стратиграфической комиссии по центру и югу Русской платформы. 2012. Вып. 5. С. 49–82].

Griffin W.L., Powell W.J., Pearson N.J., O'Reilly S.Y., 2008. GLITTER: Data Reduction Software for Laser Ablation ICP-MS. In: P.J. Sylvester (Ed.), Laser Ablation ICP-MS in the Earth Sciences: Current Practices and Outstanding Issues. Mineralogical Association of Canada Short Course Series. Vol. 40. Vancouver, p. 308–311.

Guynn J., Gehrels G., 2010. Comparison of Detrital Zircon Age Distribution Using the K-S Test Visualization and Representation of Age-Distribution Data Histograms. Available from: https://sites.google.com/laserchron.org/arizonalaserchroncenter/home (Last Accessed January 18, 2023).

Härtel B., Jonckheere R., Wauschkuhn B., Ratschbacher L., 2021. The Closure Temperature(s) of Zircon Raman Dating. Geochronology 3 (1), 259–272. https://doi.org/10.5194/gchron-3-259-2021.

Horstwood M.S.A., Kosler J., Gehrels G., Jackson S.E., McLean N.M., Paton Ch., Pearson N.J., Sircombe K., Sylvester P., Vermeesch P., Bowring J.F., Condon D.J., Schoene B., 2016. Community-Derived Standards for LA-ICP-MS U-(Th-)Pb Geochronology – Uncertainty Propagation, Age Interpretation and Data Reporting. Geostandards and Geoanalytical Research 40 (3), 311–332. https://doi.org/10.1111/j.1751-908X.2016.00379.x.

Hoskin P.W.O., Schaltegger U., 2003. The Composition of Zircon and Igneous and Metamorphic Petrogenesis. Reviews in Mineralogy and Geochemistry 53 (1), 27–62. https://doi.org/10.2113/0530027.

Ivakhnenko M.F., 2001. Tetrapods of the East European Plakkat – the Late Paleozoic Territorial-Natural Complex. Perm, 200 p. (in Russian) [Ивахненко М.Ф. Тетраподы Восточно-Европейского плакката – позднепалеозойского территориально-природного комплекса. Пермь, 2001. 200 с.].

Kaulina T.V., Lyalina L.M., Nerovich L.I., Avedisyan A.A., Il'chenko V.L., Bocharov V.N., Nitkina E.A., 2017. Processes of Hydrothermal Change in Zircon as Manifestation of Uranium Geochemistry in Rocks (A Case Study of Skalnoye Uranium Ore Occurrence in Litsa Region, Kola Peninsula). Bulletin of the Kola Scientific Center of the Russian Academy of Sciences 3, 54–63 (in Russian) [Каулина Т.В., Лялина Л.М., Нерович Л.И., Аведисян А.А., Ильченко В.Л., Бочаров В.Н., Ниткина Е.А. Процессы гидротермального изменения в цирконе как отражение геохимии урана в породах (на примере уранового рудопроявления Скальное Лицевского района Кольского полуострова) // Вестник КНЦ РАН. 2017. № 3. С. 54–63].

Kiselev D.N., Baranov V.N., Muravin E.S. et al., 2012. Geosites of the Yaroslavl Area: Stratigraphy, Paleontology, Paleogeography. Yustitsinform, Moscow, 304 p. (in Russian) [Киселев Д.Н., Баранов В.Н., Муравин Е.С. и др. Объекты геологического наследия Ярославской области: стратиграфия, палеонтология и палеогеография. М.: Юстицинформ, 2012. 304 с].

Kuleshov V.N., Arefiev M.P., Pokrovsky B.G., 2019. Isotope Characteristics ($\delta^{13}C$, $\Delta^{18}O$) of Continental Carbonates from Permian – Triassic Rocks in the Northeastern Russian Plate: Paleoclimatic and Biotic Reasons and Chemostratigraphy. Lithology and Mineral Resources 54, 489–510. https://doi.org/10.1134/S0024490219060075.

Kuznetsov N.B., Belousova E.A., Alekseev A.S., Romanyuk T.V., 2014a. New Data on Detrital Zircons from the Sandstones of Lower Cambrian Brusov Formation (White-Sea Region, East-European Craton): Unraveling the Timing of the Onset of the Arctida-Baltica Collision. International Geology Review 56 (16), 1945–1963. https://doi.org/10.1080/00206814.2014.977968.

Kuznetsov N.B., Meert J.G, Romanyuk T.V., 2014b. Ages of the Detrital Zircons (U/Pb, La-ICP-MS) from Latest Neoproterozoic – Middle Cambrian(?) Asha Group and Early Devonian Takaty Formation, the South-Western Urals: A Testing of an Australia-Baltica Connection within the Rodinia. Precambrian Research 244, 288–305. https://doi.org/10.1016/j.precamres.2013.09.011.

Linnemann U., Ouzegane K., Drareni A., Hofmann M., Becker S., Gärtner A., Sagawe A., 2011. Sands of West Gondwana: An Archive of Secular Magmatism and Plate Interactions – A Case Study from the Cambro-Ordovician Section of the Tassili Ouan Ahaggar (Algerian Sahara) Using U-Pb-LA-ICP-MS Detrital Zircon Ages. Lithos 123 (1–4), 188–203. https://doi.org/10.1016/j.lithos.2011.01.010.

Lozovsky V.R., Balabanov Y.P., Karasev E.V., Novikov I.V., Ponomarenko A.G., Yaroshenko O.P., 2016. The Terminal Permian in European Russia: Vyaznikovian Horizon, Nedubrovo Member, and Permian–Triassic Boundary. Stratigraphy and Geological Correlation 24, 364–380. https://doi.org/10.1134/S0869593816040043.

Lozovsky V.R., Esaulova N.K. (Ed.), 1998. The Permian-Triassic Boundary in the Continental Series of Eastern Europe. In: Upper Permian Stratotypes of the Volga Region. Proceedings of the International Symposium. GEOS, Moscow, 246 p. (in Russian) [Граница перми и триаса в континентальных сериях Восточной Европы // Верхнепермские стратотипы Поволжья: Материалы к Международному симпозиуму / Ред. В.Р. Лозовский, Н.К. Есаулова. М.: ГЕОС, 1998. 246 с].

Lozovsky V.R., Novikov I.V., 2016. Stratigraphic Scheme of the Triassic of Moscow and Mezen Syneclises: State-of-Art and Problems. In: State of the Stratigraphic Base of the Center and Southeast of the East European Platform. Proceedings of Meeting (November 23–25, 2015). VNIGRI, Moscow, p. 80–87 (in Russian) [Лозовский В.Р., Новиков И.В. Стратиграфическая схема триасовых отложений Московской и Мезенской синеклиз: состояние и проблемы // Состояние стратиграфической базы центра и юго-востока Восточно-Европейской платформы: Материалы совещания (23–25 ноября 2015 г.). М.: ВНИГРИ, 2016. С. 80–87].

Mints M.V., 2017. Meso-Neoproterozoic Grenville-Sveconorwegian Intracontinental Orogen: History, Tectonics, Geodynamics. Geodynamics & Tectonophysics 8 (3), 619–642 (in Russian) [Минц М.В. Мезонеопротерозойский Гренвилл-Свеконорвежский внутриконтинентальный ороген: история, тектоника, геодинамика // Геодинамика и тектонофизика. 2017. Т. 8. № 3. С. 619–642]. https://doi.org/10.5800/GT-2017-8-3-0309.

Nasdala L., Wenzel M., Vavra G., Irmer G., Wenzel T., Kober B., 2001. Metamictisation of Natural Zircon: Accumulation versus Thermal Annealing of Radioactivity-Induced Damage. Contributions to Mineralogy and Petrology 141, 125–144. https://doi.org/10.1007/s004100000235.

Pastor-Galán D., Nance R.D., Murphy J.B., Spencer C.J., 2019. Supercontinents: Myths, Mysteries, and Milestones. Geological Society of London Special Publications 470 (1), 39–64. https://doi.org/10.1144/SP470.16.

Paton Ch., Hellstrom J.C., Paul P., Woodhead J.D., Hergt J.M., 2011. Iolite: Freeware for the Visualisation and Processing of Mass Spectrometric Data. Journal of Analytical Atomic

Spectrometry 26, 2508–2518. https://doi.org/10.1039/C1JA10172B.

Petrov O.V. (Ed.), 2012. Geological Map of Russia and Adjacent Water Areas. Scale 1:2500000. VSEGEI Publishing House, Saint Petersburg (in Russian) [Геологическая карта России и прилегающих акваторий. Масштаб 1:2500000 / Ред. О.В. Петров. СПб.: Изд-во ВСЕГЕИ, 2012].

Pidgeon R.T., 2014. Zircon Radiation Damage Ages. Chemical Geology 367, 13–22. https://doi.org/10.1016/j.chemgeo.2013.12.010.

Powerman V.I., Buyantuev M., Ivanov A.V., 2021. A Review of Detrital Zircon Data Treatment, and Launch of a New Tool "Dezirteer" along with the Suggested Universal Workflow. Chemical Geology 583, 120437. https://doi.org/10.1016/j.chemgeo.2021.120437.

Puchkov V.N., 2010. Geology of the Urals and Cisurals (Topical Issues of Stratigraphy, Tectonics, Geodynamics and Metallogeny). DizaynPoligrafServis, Ufa, 280 p. (in Russian) [Пучков В.Н. Геология Урала и Приуралья (актуальные вопросы стратиграфии, тектоники, геодинамики и металлогении). Уфа: ДизайнПолиграфСервис. 2010. 280 с.].

Pystin A.M., Ulyasheva N.S., Pystina Y.I., Grakova O.V., 2020. Provenance and U-Pb Age of Detrital Zircons from the Upper Proterozoic Deposits of the Polar Urals: To the Question of the Time of Formation of the Timan Passive Margin. Stratigraphy and Geological Correlation 28 (5), 457–478. https://doi.org/10.1134/S0869593820050081.

Resentini A., Andò S., Garzanti E., Malusà M.G., Pastore G., Vermeesch P., Chanvry E., Dall'Asta M., 2020. Zircon as a Provenance Tracer: Coupling Raman Spectroscopy and U-Pb Geochronology in Source-To-Sink Studies. Chemical Geology 555, 119828. https://doi.org/10.1016/j.chemgeo.2020.119828.

Sláma J., Košler J., Condon D.J., Crowley J.L., Gerdes A., Hanchar J.M., Horstwood M.S.A., Morris G.A. et al., 2008. Plešovice Zircon – A New Natural Reference Material for U-Pb and Hf Isotopic Microanalysis. Chemical Geology 249 (1–2), 1–35. https://doi.org/10.1016/j.chemgeo.2007.11.005.

Soboleva A.A., Kuznetsov N.B., Miller E.L., Udoratina O.V., Gehrels G., Romanyuk T.V., 2012. First Results of U-Pb Dating of Detrital Zircons from Basal Horizons of Uralides (Polar Urals). Doklady Earth Sciences 445, 962–968. https://doi.org/10.1134/S1028334X12080156.

Strok N.I., Trofimova I.S., 1976. Influence of the Ural and Baltic Provenances on the Formation of the Upper Permian and Lower Triassic Sequences of the Moscow Syneclise. Bulletin of Moscow Society of Naturalists. Geological Series 51 (1), 100–110 (in Russian) [Строк Н.И., Трофимова И.С. Влияние уральской и балтийской питающих провинций на формирование верхнепермских и нижнетриасовых отложений Московской синеклизы // Бюллетень МОИП. Отдел геологический. 1976. Т. 51. № 1. С. 100–110].

Vermeesch P., 2013. Multi-Sample Comparison of Detrital Age Distributions. Chemical Geology 341, 140–146. https://doi.org/10.1016/j.chemgeo.2013.01.010.

Vermeesch P., 2018. IsoplotR: A Free and Open Toolbox for Geochronology. Geoscience Frontiers 9 (5), 1479–1493. https://doi.org/10.1016/j.gsf.2018.04.001.

Veselovskiy R.V., Dubinya N.V., Ponomarev A.V., Fokin I.V., Patonin A.V., Pasenko A.M., Fetisova A.M., Matveev M.A., Afinogenova N.A., Rud'ko D.V., Chistyakova A.V., 2022. Shared Research Facilities "Petrophysics, Geomechanics and Paleomagnetism" of the Schmidt Institute of Physics of the Earth RAS. Geodynamics & Tectonophysics 13 (2), 0579 (in Russian) [Веселовский Р.В., Дубиня Н.В., Пономарев А.В., Фокин И.В., Патонин А.В., Пасенко А.М., Фетисова А.М., Матвеев М.А., Афиногенова Н.А., Рудько Д.В., Чистякова А.В. Центр коллективного пользования Института физики Земли им. О.Ю. Шмидта РАН «Петрофизика, геомеханика и палеомагнетизм» // Геодинамика и тектонофизика. 2022. Т. 13. № 2. 0579.]. https://doi.org/10.5800/GT-2022-13-2-0579.